Design of a Soil Vapor Barrier to Prevent Gas Diffusion from Waste Dumps

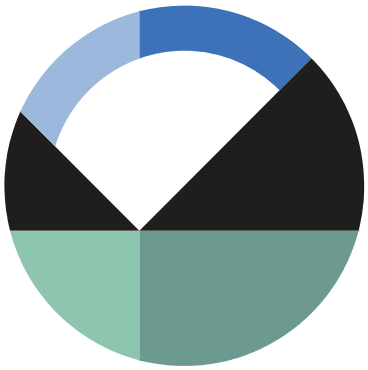

GEO-SLOPE International Ltd. | www.geo-slope.com

1200, 700 - 6th Ave SW, Calgary, AB, Canada T2P 0T8
Main: +1 403 269 2002 | Fax: +1 888 463 2239

Introduction

Capillary soil covers comprise a tension saturated layer that can be used to restrict oxygen ingress into waste materials that contain reactive substances. Alternatively, capillary covers can be used to restrict movement into the atmosphere of gases generated by the waste materials. Barbour et al. (2005) describe an example of the latter case in which a capillary cover that was constructed to limit transport of volatile organic compounds (VOCs) generated by pulverized fuel ash at a former industrial site in South Wales.

The numerical model associated with this example simulates the water dynamics and gas transfer within the capillary barrier and waste materials subject to different climate and vegetation conditions. The land-climate-interaction (LCI) boundary condition in SEEP/W is used to calculate the infiltration flux at each point in time from the precipitation, evaporation, and runoff. The LCI boundary condition also calculates water uptake within the root zone in accordance with potential evapotranspiration flux and water stresses within the ground. The resulting water distribution is then used in the CTRAN/W analysis to simulate gas transfer by hydrodynamic dispersion through both the air and dissolved phases.

Background

Barbour et al. (2005) discuss the design of a soil cover over a pulverized fuel ash (PFA) waste site located in an urban area in South Wales. Other waste streams were also present within the dump, leading to the potential for the generation of volatile and semi-volatile organic compounds (VOCs and SVOCs). Remediation of the area required that gas movement into the atmosphere be restricted.

Soil cover systems are built upon various types of waste dumps and are designed to prevent either water movement into the waste or gas/vapor movement into the atmosphere. The use of a capillary break and moisture retaining layer within a soil cover system is one design that limits the upward migration of gas or vapors from the underlying waste into the atmosphere. The movement of gas or vapors occurs through a combination of advection and diffusion, with the advective processes becoming negligible if the degree of saturation remains at greater than 85%. Diffusion processes are also highly restricted as the soil nears saturation because the coefficient of diffusion in the air phase is more than 3 orders of magnitude larger than in the water phase (Barbour et al. 2005).

Barbour (1990) described the influence of coarser and finer layers under varying rates of infiltration on the overall degree of saturation throughout the soil profile. A fine layer of soil surrounded by coarse layers results in the fine layer remaining saturated, even under negative pore-water pressure (Figure 1). To ensure that the fine layer remains saturated, the air-entry value of the fine layer soil must be greater than the suction at which the coarse layer reaches the residual water content. The surface evaporation or evapotranspiration must also be considered when designing the soil cover system to ensure that the fine layer does not dry out because of demands of vegetation or evaporation on the soil cover (Barbour et al. 2005).

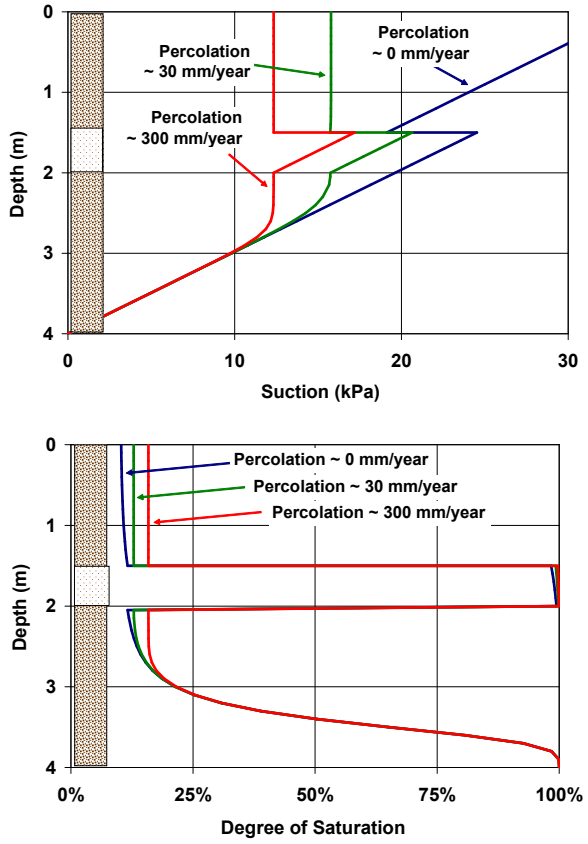

Figure 1. Suction and saturation profiles for varying percolation rates (Barbour et al. 2005).

Numerical Simulation

One-dimensional water transfer analyses were used to determine if the water retention layer within the capillary barrier remains tension saturated when subject to certain climate conditions and vegetation scenarios. Two 0.05 m thick layers of Quarry dust were proposed to produce capillary breaks on either side of a 0.2 m thick water retaining layer formed by PFA (Figure 2). The capillary barrier is underlain by 0.15 m of 6 mm stone and overlain by 1.25 m of coarse top soil and 0.3 m layer of a fine top soil, forming a total cover thickness of 2 m (Figure 2). Three different scenarios were considered (Barbour et al., 2005): a) normal climate conditions and grass growth (Case 1a); b) normal climate conditions and tree growth (Case 1b); and c) a dry climate year and tree growth (Case 2).

Barbour et al. (2005) simulated liquid water flow and vapor transfer in response to pore-water pressure and temperature gradients. Liquid water transfer is, however, the dominate process for these test cases; consequently, the vapor transfer processes were not simulated. Additional numerical simulations could be completed by toggling on the optional isothermal and/or thermal vapor transfer physics. The later process requires simulation of the heat transfer processes in addition to the water transfer dynamics.

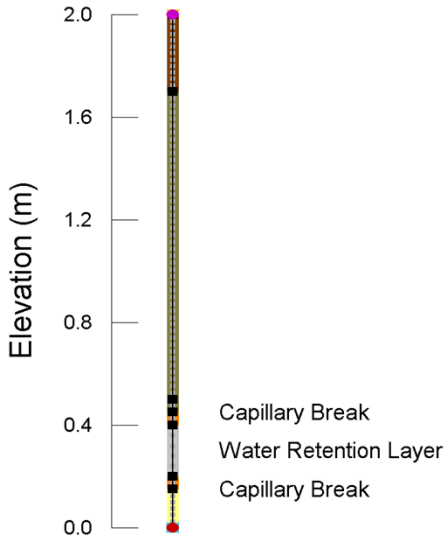

Figure 2. Numerical model domain.

The hydraulic properties of each of the materials were presented by Barbour et al. (2005). The volumetric water content and hydraulic conductivity functions for each material in the cover are shown in Figure 3 and Figure 4, respectively.

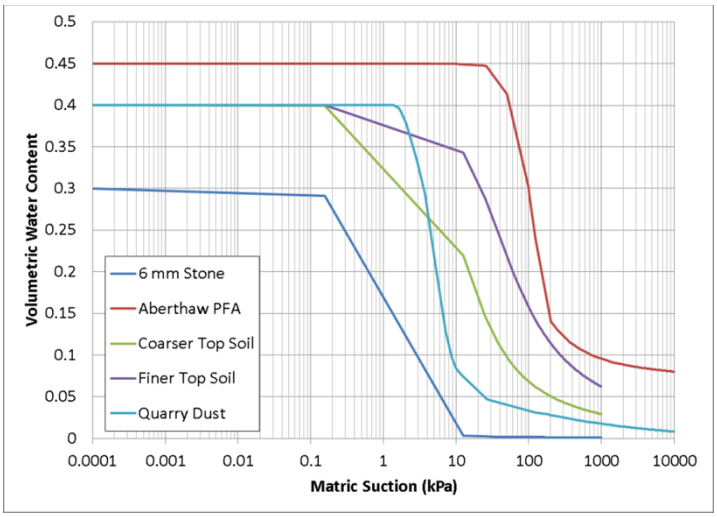

Figure 3. Volumetric water content functions for each material used in the analyses.

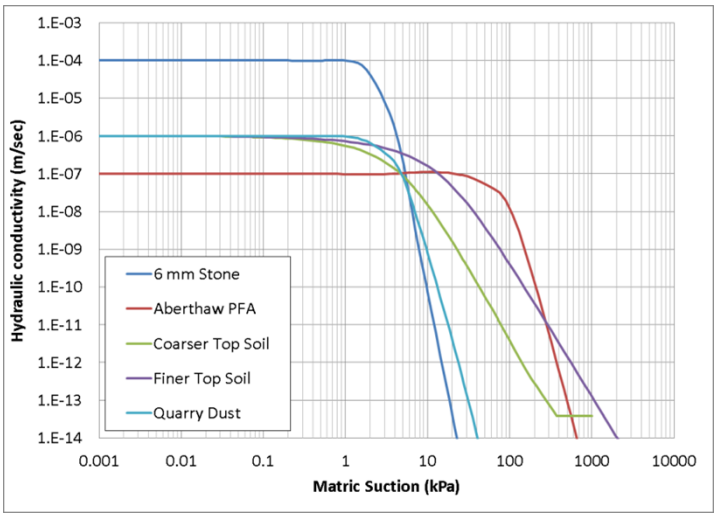

Figure 4. Hydraulic conductivity functions for each material used in the analyses.

The gas transfer analysis is conceptual in nature. The gases in the waste materials were VOC; however, the properties for the gas were assumed to be those of carbon dioxide (CO_2). The coefficient of diffusion in the gas phase was assumed to be 1.64 x 10^{-5} m^2/sec in dry soil, while the coefficient of gas transport in the dissolved phase was assumed to be 1.60 x 10^{-9} m^2/sec. The solubility coefficient was defined as 0.83 with an activation concentration of 0 Mg/m^3. The longitudinal and transverse dispersivities in the water phase are defined as 3 x 10^{-3} and 3 x 10^{-4} m.

The two climate conditions that were chosen by Barbour et al. (2005) were the years 1989 and 1996 for the dry and normal climate conditions, respectively. The climate data was taken from the Cardiff weather data set for 1989, which was scaled to modify the precipitation and potential evaporation data to match those experienced at the Cardiff weather station and the MET office in the study site area during the simulation years (Barbour et al., 2005). Figure 5, Figure 6, and Figure 7 show the air temperature, wind speed, and relative humidity functions that were used in the LCI boundary

condition for all analyses. Figure 8 and Figure 9 show the cumulative precipitation and potential evapotranspiration (PET) for the normal and dry years, respectively.

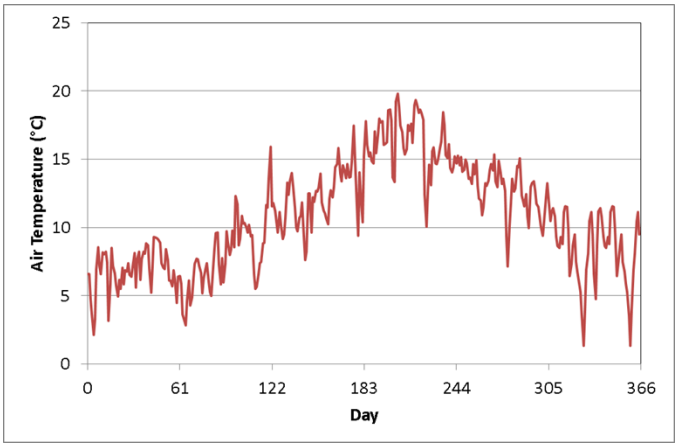

Figure 5. Average daily air temperature function.

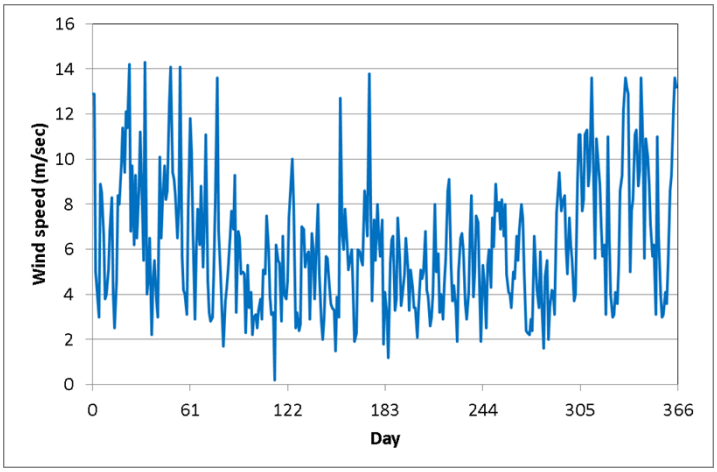

Figure 6. Average daily wind speed function.

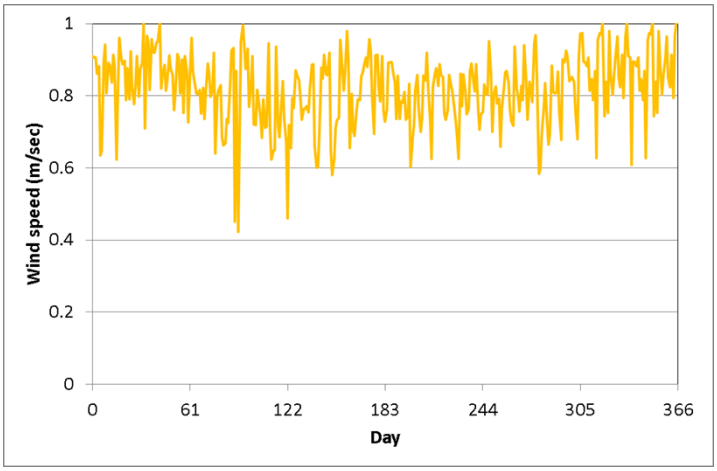

Figure 7. Average daily relative humidity function.

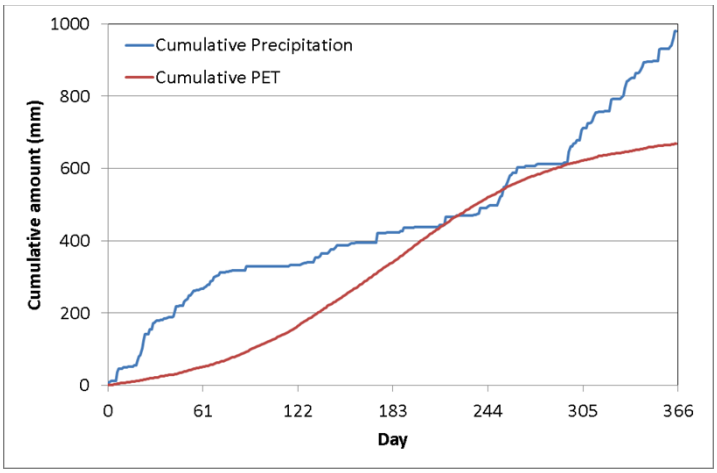

Figure 8. Cumulative precipitation and evapotranspiration functions for the normal climate year (Case 1).

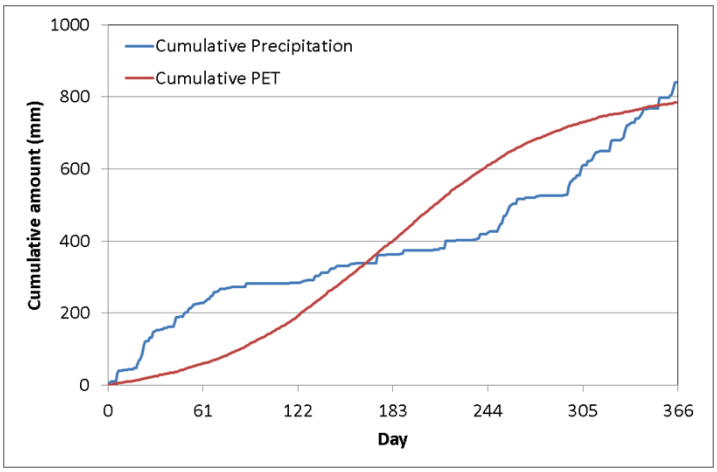

Figure 9. Cumulative precipitation and evapotranspiration functions for the dry climate year (Case 2).

The vegetation data set was developed for grass and tree growth. Barbour et al. (2005) assumed a leaf area index (LAI) for both vegetation types of 2.7 throughout the year, which is the LAI at which maximum transpiration is reached. The vegetation height was assumed to reach a maximum of 1m for both vegetation types, while the root depth was assumed to be 1m for tree growth and 0.25 m for grass growth. It was assumed that transpiration would be unrestricted at soil suctions less than 100 kPa, while the limiting factor decreased in proportion to the matric suction until the permanent wilting point of 1500 kPa was reached and transpiration is negligible. The root density and soil cover fraction functions were estimated based on Prasad (1998) and Ritchie (1972), respectively, and are shown in Figure 10 and Figure 11.

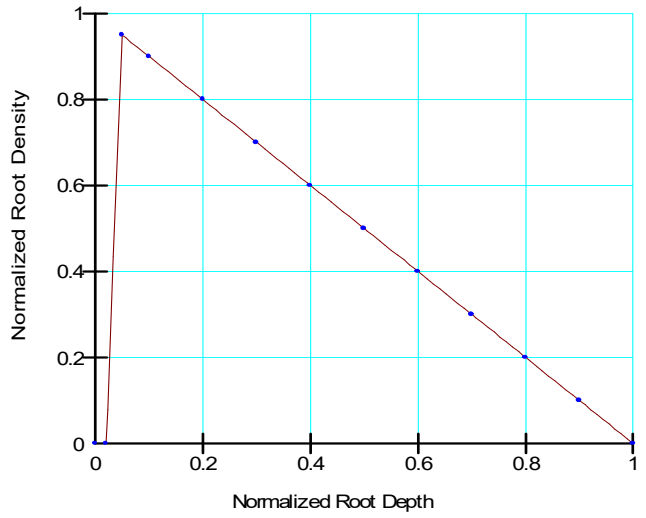

Figure 10. Normalized root density function without roots in the upper 5 cm based on Prasad (1998).

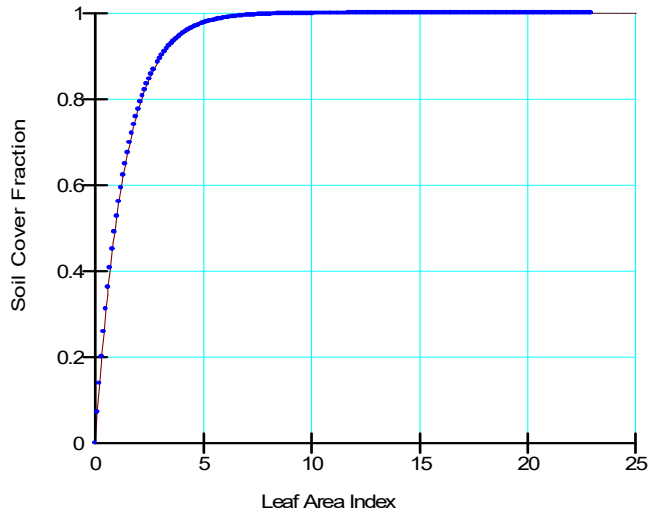

Figure 11. Soil cover fraction function based on Ritchie (1972).

The lower 6 mm stone material at the base of the cover is assumed to act as a 'leakage' boundary, indicating that a drip surface must develop prior to water being able to cross the lower boundary (Barbour et al., 2005). Since the water table depth is assumed to be below the soil cover, a unit gradient boundary condition is placed on the bottom node of the one-dimensional column. Gas boundary conditions of 1 Mg/m^3 and 0 Mg/m^3 are defined at the bottom and the top of the column, respectively.

The initial pore-water pressure conditions are defined using spatial functions. The same three analyses were simulated for a total duration of 3 years each to remove the influence of the initial pore-water pressure conditions on the response of the profile to climatic conditions. The final pore-

water pressure profile on the last day of each "spin-up" was used to create the spatial functions for each analysis. Each analysis simulates the full climate year with 2 hour time step increments. The analyses save every 12 steps or 1 day time steps.

Results and Discussion

The net percolation through the 2 m cover was the greatest in Case 1a, with a cumulative net percolation of approximately 477 mm (Figure 12). The net percolation decreases with the introduction of tree growth, with the least amount observed Case 2, with a cumulative net percolation of approximately 195 mm.

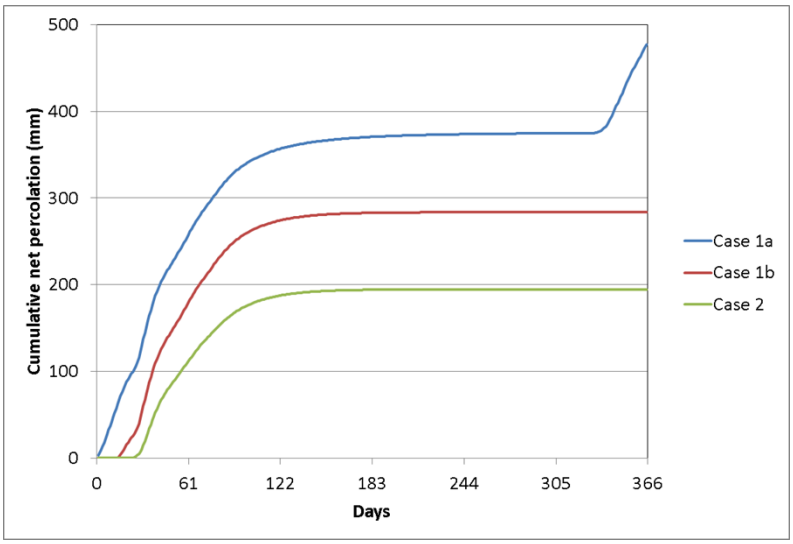

Figure 12. Net percolation leaving the cover for each analysis.

For the normal climate year in Case 1, the cumulative precipitation and PET was defined as 980 mm and 670 mm, respectively. For Case 1a, actual evaporation and transpiration were simulated as 49 mm and 463 mm, for a total actual evapotranspiration of 512 mm or 76% of the PET (Figure 13). For Case 1b, the actual evaporation and transpiration was simulated as 58 mm and 488 mm, respectively, for a total evapotranspiration of 546 mm or 81% of the PET (Figure 14).

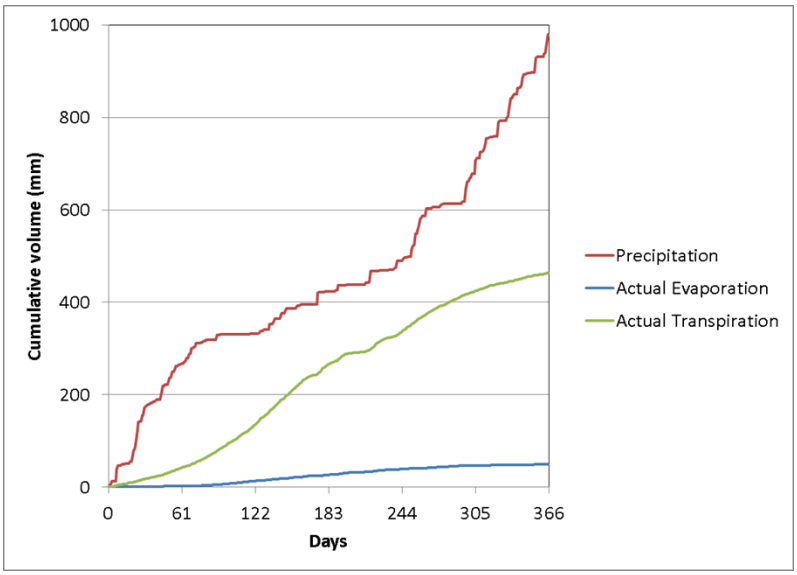

Figure 13. Simulated evaporation, transpiration and precipitation for Case 1a.

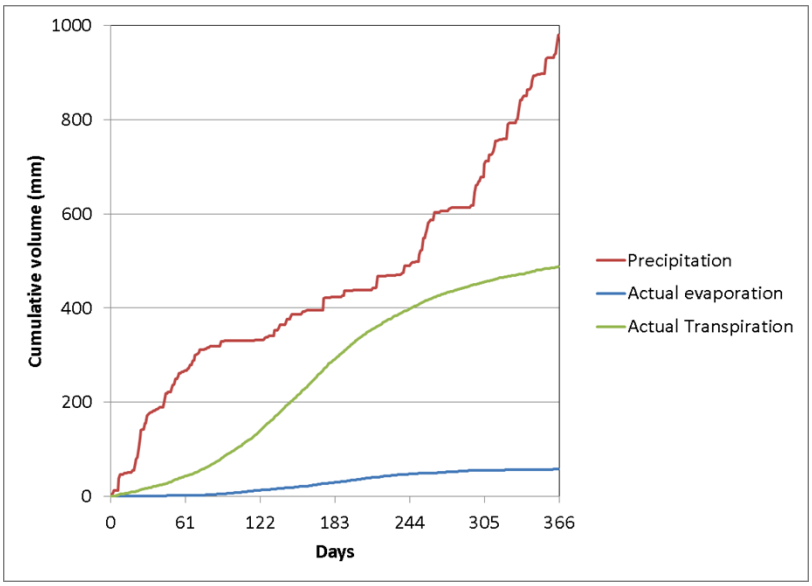

Figure 14. Simulated evaporation, transpiration and precipitation for Case 1b.

In Case 2, the PET applied in the LCI boundary condition increases to approximately 785 mm, with a total precipitation of only 840 mm. The actual evaporation and transpiration simulated are 64 mm and 497 mm, for a total simulated evapotranspiration of 561 mm, or 71% of the PET (Figure 15).

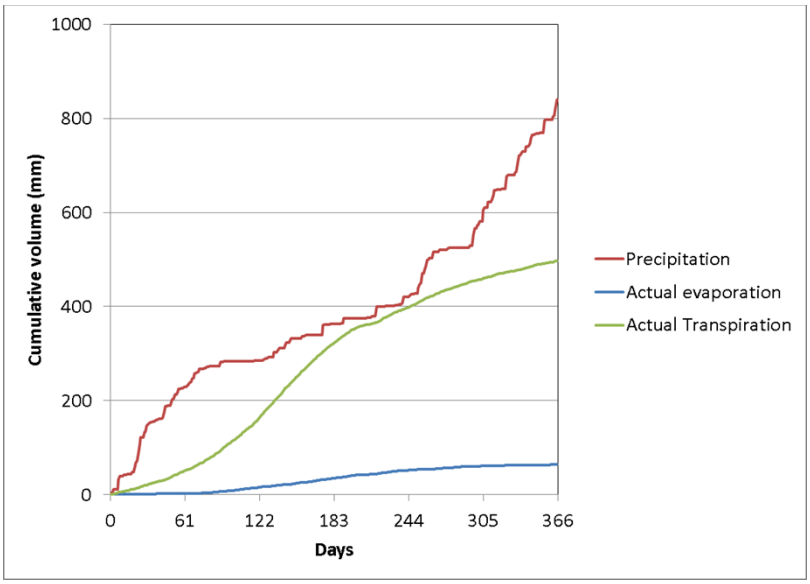

Figure 15. Simulated evaporation, transpiration and precipitation for Case 2.

In all three analyses, the water retention layer was able to remain saturated at the saturated water content of 0.45 throughout the simulation year. The volumetric water content (VWC) profiles throughout the simulation year for Cases 1a, 1b and 2 are shown in Figure 16, Figure 17, and Figure 18, respectively.

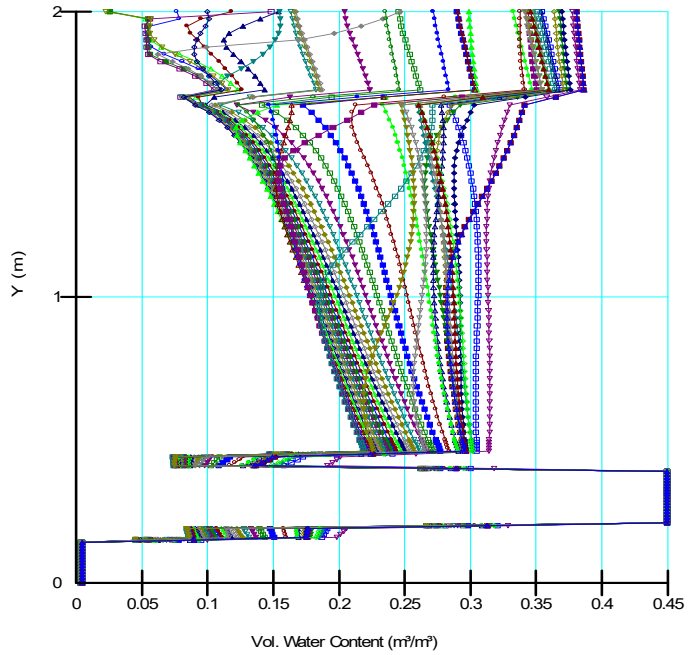

Figure 16. VWC profile throughout the year in Case 1a.

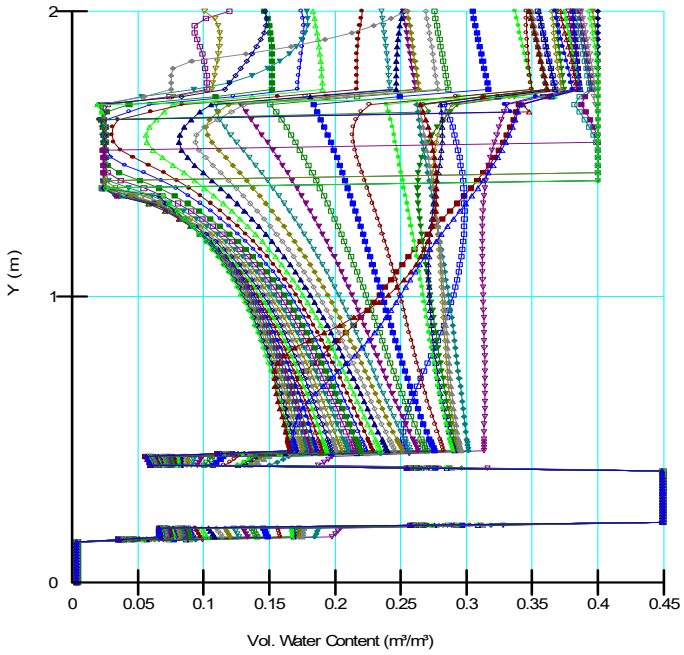

Figure 17. VWC profile throughout the year in Case 1b.

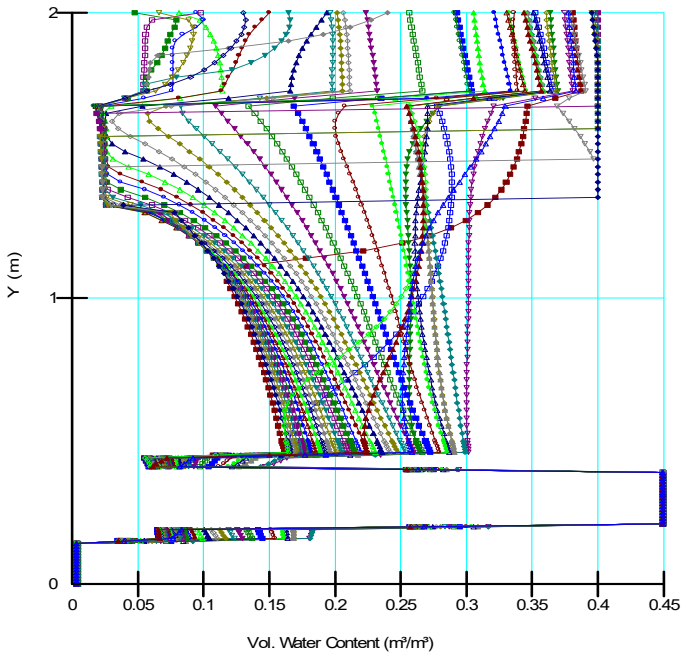

Figure 18. VWC profile throughout the year in Case 2.

The movement of gas up the soil cover in Case 1a is limited during parts of the year where water is flowing downward through the soil cover (Figure 19). As the net percolation rate slows, and the evaporation and transpiration rates increase, upward gas movement through the soil cover begins. This causes an increase in the mass of CO_2 experienced above the moisture retaining layer of the soil

cover. During the early winter season, infiltration rates into the moisture retaining layer increase, thus causing a decrease in the CO_2 mass accumulating above the soil capillary barrier.

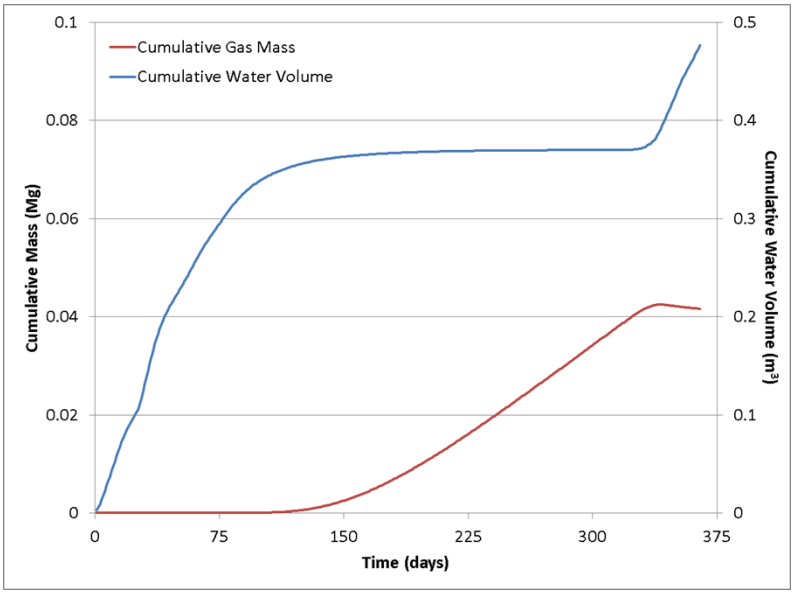

Figure 19. Cumulative mass of CO_2 and cumulative water volume versus time above the moisture retaining layer in Case 1a.

Similar patterns are observed in Case 1b and 2 (Figure 20 and Figure 21), but the cumulative gas mass continues to increase toward the end of the year, where infiltration into the moisture retaining layer does not increase as shown in Case 1a. As water is removed from the upper portion of the column from evapotranspiration, the CO_2 is transported up the column at a faster rate. As the cumulative water volume entering the moisture retaining layer decreases, the cumulative mass of gas increases with the highest accumulative of gas occurring in Case 2.

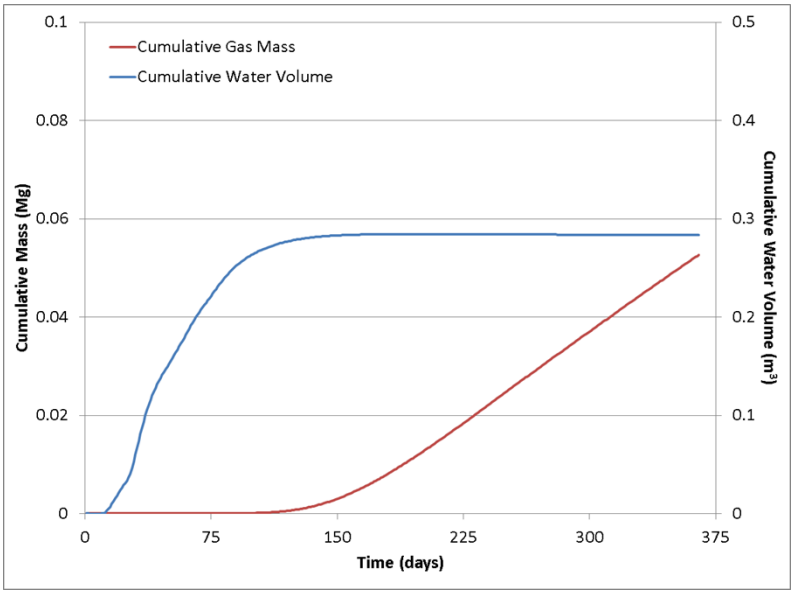

Figure 20. Cumulative mass of CO_2 and cumulative water volume versus time above the moisture retaining layer in Case 1b.

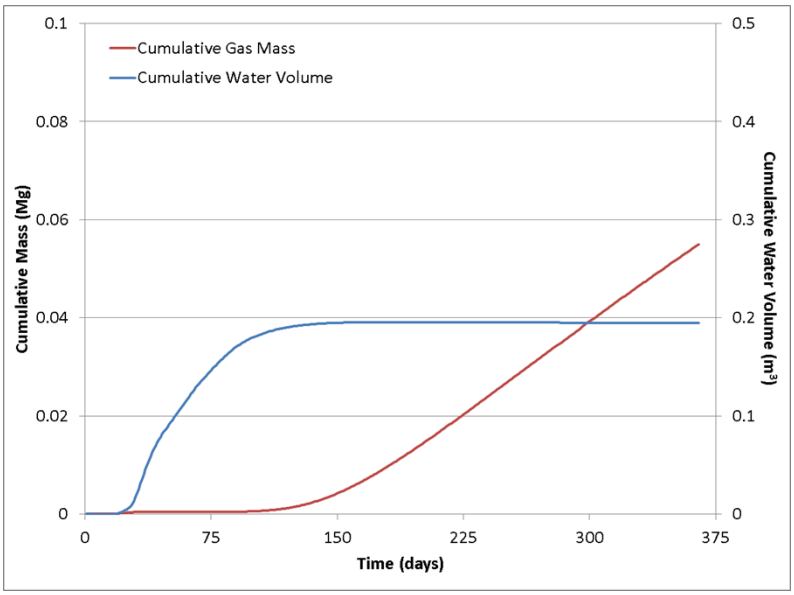

Figure 21. Cumulative mass of CO_2 and cumulative water volume versus time above the moisture retaining layer in Case 2.

Summary and Conclusions

A cover system was simulated under three different climate and vegetation scenarios to illustrate the use of a moisture retaining layer on reducing the upward gas movement from a waste dump. The moisture retaining layer surrounded by capillary breaks was able to stay saturated throughout each of the analysis years. This reduced the accumulation of gas mass experienced in the upper layers of the soil cover. The resulting net percolation and actual evapotranspiration rates experienced in this example are similar to those presented by Barbour et al. (2005).

References

Barbour, S.L. 1990. Discussion of "Reduction of acid generation in mine tailings through the use of moisture-retaining cover layers as oxygen barriers." Canadian Geotechnical Journal 27 (3): 398-401.

Barbour, S.L., Sladen, J. and Wright, I. 2006. The design and construction of a soil vapor barrier in Caerphilly, South Wales, UK. Canadian Geotechnical Society Conference, Saskatoon, Saskatchewan, September 18-21.

Prasad R. 1988. A linear root water uptake model. Journal of Hydrology. Volume 99: 297–306.

Ritchie, J.T. 1972. Model for predicting evaporation from a row crop with incomplete cover. Water Resources Research. Volume 8 (5): 1204-1213.